Physica E 43 (2010) 155–160

Contents lists available at ScienceDirect

Physica E

journal homepage: www.elsevier.com/locate/physe

# Geometry and temperature dependent thermal conductivity of diamond nanowires: A non-equilibrium molecular dynamics study

Jing Guo [a], Bin Wen [a,b,*], Roderick Melnik [c,d], Shan Yao [a], Tingju Li [a]

[a] School of Materials Science and Engineering, Dalian University of Technology, Dalian 116023, China
[b] State Key Laboratory of Metastable Materials Science and Technology, Yanshan University, Qinhuangdao 066004, China
[c] M²NeT Lab, Wilfrid Laurier University, Waterloo, 75 University Avenue West, Ontario, Canada N2L 3C5
[d] BCAM, Bizkaia Technology Park, 48160 Derio, Spain

ARTICLE INFO

*Article history:*
Received 18 November 2009
Received in revised form
25 June 2010
Accepted 29 June 2010
Available online 23 July 2010

ABSTRACT

Using non-equilibrium molecular dynamics methods, the analysis of geometry and temperature dependent thermal conductivities of diamond nanowires is carried out. It is found that at the same temperature conditions, thermal conductivities of diamond nanowires increase with increasing lengths, ranging from 20 to 350 nm and cross-sectional areas ranging from 2 to 30 $nm^2$. At the same length, temperature and cross-sectional area conditions, thermal conductivities of $\langle 0\,1\,1 \rangle$ crystal orientation diamond nanowires are larger than those of other crystal orientation diamond nanowires. First, in the temperature range 0–1000 K, thermal conductivities of diamond nanowires increase with the increase in temperature, and then they decrease. The results of our calculation have also indicated that all thermal conductivities of the diamond nanowires analyzed here are smaller than those of the corresponding orientations in bulk diamond. Finally, a relationship between thermal conductivity and density of phonon state is discussed.



## 1. Introduction

Due to their unique quantum properties and potential applications as nanocomposites for mechanical reinforcement and thermal management, diamond nanowires (DNWs) have become an important object of investigations [1–5]. Diamond nanowires were synthesized for the first time in 1997 by Shiomi [6]. After that, DNWs have been fabricated by various methods [7–12], including those based on air plasma etching of polycrystalline diamond films [7], microwave plasma assisted chemical vapor deposition [8], reactive ion etching of single crystal diamond substrates [9], hydrogen plasma etching of multiwalled carbon nanotubes [10,11] and hydrogen/argon plasma etching of Au nanodots [12].

In addition to the fabrication of DNWs, intense theoretical and experimental efforts have been focused on the mechanical and chemical properties of DNWs. For example, orientation dependent brittle fracture forces and stiffnessess have been studied using first principles calculations by Shenderova et al. [13]. Surface morphology, surface hydrogenation and diameter dependent energy band gap have also been investigated using first principles calculations by Barnard [14]. Scratching experiments have been performed to study the mechanical properties of aggregated DNWs by Dubrovinskaia et al. [15]. Electrochemical sensor experiments have been carried out by Nebel et al. [16].

In many applications of DNWs, their thermal conductive properties become a key issue. However, for nanoscale materials, it is difficult to carry out a thermal conductivity measurement experimentally. Up to date, there are no experimental reports on DWNs thermal conductivity. For theoretical calculations of properties of nanosized diamond materials, polycrystalline diamond thin films' thermal conductivity has been analyzed using the Klemens–Callaway's expression (e.g. [17]). Diamond thin films thermal conductivity has also been investigated using the molecular dynamics method by Wu et al. [18]. Carbon nanotubes and diamond nanowire thermal conductivities have been studied by atomistic simulations in the works of Moreland et al. [19,20]. Diamond nanorod's thermal conductivity has also been calculated by the molecular dynamics method by Padgett et al. [5]. Diamond nanoparticle's thermal conductivity has been investigated by the molecular dynamics method by Li et al. [21]. However, to the best of our knowledge, geometry and temperature dependent thermal conductivity of diamond nanowires has not been studied to date in detail. To fill this gap, in this work, geometry and temperature dependent thermal conductivity of diamond nanowires will be studied using a non-equilibrium molecular dynamics method [22].

## 2. Computational method

By comparing the nearest neighbor separation of 1.54 Å for diamond to its de Broglie thermal wavelength, known to be 0.2899 Å at 300 K, the effectiveness of the classical molecular

* Corresponding author at: School of Materials Science and Engineering, Dalian University of Technology, Dalian 116023, China.
*E-mail address:* wenbin@dlut.edu.cn (B. Wen).

1386-9477/$ - see front matter © 2010 Elsevier B.V. All rights reserved.
doi:10.1016/j.physe.2010.06.032

dynamics method approximation has been demonstrated by a number of authors (e.g. [23]). Quantum disturbances in this case can be neglected. Therefore, DNWs thermal conductivity has been calculated using a non-equilibrium molecular dynamics method [22] and no quantum effects have been considered in this work. A schematic representation of the system we simulate is shown in Fig. 1(a). As can be seen, the cuboid represents the DNWs. To obtain temperature for different positions, DNWs were divided into $n$ equal slabs along the $z$ direction, and we called the first slab and the last slab as "hot" and "cold" slabs, respectively. In order to produce a simulated constant heat flux in the system, heat $\Delta E$ was added to the "hot" slab and the same heat $\Delta E$ was removed from the "cold" slab by rescaling velocities at every simulation time step. Therefore, the simulated constant heat flux can be expressed as

$$J_Z = \frac{\Delta E}{\Delta t A} \tag{1}$$

where $\Delta t$ is the simulation time step and $A$ is cross-sectional area perpendicular to the $z$ direction.After thermodynamic equilibrium is reached, the temperature at different positions can be obtained by computing atoms velocity $v$ at the corresponding slabs. Hence, the temperature in the $m$th slab $T^m_{slab}$ can be expressed as

$$T^m_{slab} = \frac{1}{3Nk_B}\sum_{i=1}^{N} m_k v_k^2 \tag{2}$$

where $N$ is the number of atoms in the slab and $k_B$ is Boltzmann's constant. Then the temperature gradient in the $z$ direction, $G_z$, in the position of the $m$th slab can be expressed as

$$G_z = \frac{n(T^{m+1}_{slab} - T^{m-1}_{slab})}{2l} \tag{3}$$

where $T^{m+1}_{slab}$ and $T^{m-1}_{slab}$ are the temperatures in the positions of slabs $m+1$ and $m-1$, respectively and $l$ is the length of the DNWs. Using Fourier's law

$$J_z = -k_z G_z \tag{4}$$

where $J_z$ is the heat flux in the $z$ direction and $G_z$ the temperature gradient, and thermal conductivity in the $z$ direction, $k_z$, can be written as

$$k_z = \frac{2l\Delta E}{n\Delta t A(T^{m+1}_{slab} - T^{m-1}_{slab})} \tag{5}$$

In this contribution, molecular dynamics (MD) calculations have been performed by employing the widely used Large-scale Atomic/Molecular Massively Parallel Simulator (LAMMPS) package [24]. In our computational scheme, C–C bonding interactions are described by the Tersoff potential [25], NPT ensemble is used and the pressure is the atmospheric pressure. Simulated input heat $\Delta E$ is 0.01 eV, and the simulation step time is 2 fs. The entire simulation time is 2 ns, which is $1\times10^6$ MD steps. Our simulation results indicated that simulation time of 2 ns is sufficient to equilibrate the nanostructure. For example, a relationship between temperature and simulation time (or time steps) for bulk diamond is shown in Fig. 1(b). This result indicates that $4\times10^5$ MD steps are sufficient to reach the steady state, and similar results hold true for all DNWs studied in this work. For different length DNWs, 15–40 slabs are required. Our simulation results have also indicated that 15–40 slabs are sufficient to obtain the temperature with necessary accuracy.

To verify the accuracy, bulk diamond thermal conductivities in the temperature range 0–1000 K have been investigated using this method. As can be seen from Fig. 2, good agreement results have been obtained when comparing our simulated values with known experimental and other theoretical results [17,26,27]. This indicates that our computational method and parameters are suitable for thermal conductivity calculations. We also note that similar methodologies have already been applied successfully to the analysis of several other nanostructures [28–47].

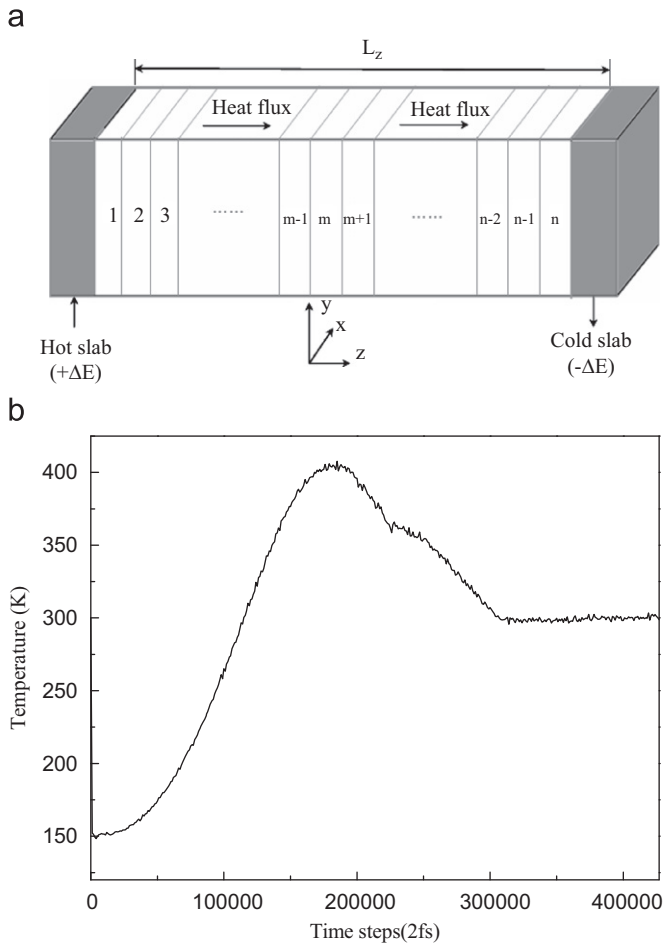


**Fig. 1.** (a) A schematic representation of the simulated system and (b) a relationship between temperatures and time steps for bulk diamond at the temperature of 300 K.

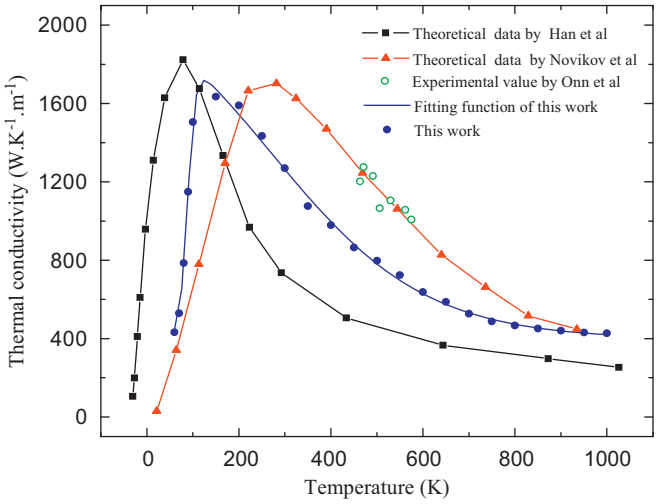


**Fig. 2.** Bulk diamond thermal conductivities computed in this work in the temperature range 0–1000 K. The corresponding theoretical and experimental data are given in Ref. [17, 26, 27].

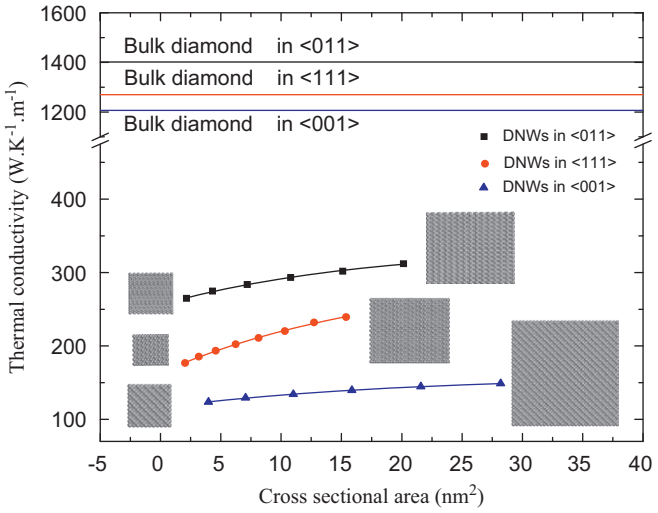


**Fig. 3.** DNW thermal conductivities with cross-sectional areas ranging from 2 to 30 nm$^2$ and length 85.6 nm at 300 K in the ⟨0 1 1⟩, ⟨1 1 1⟩ and ⟨0 0 1⟩ crystal orientations. Also shown are data of bulk diamond computed in this simulation. The insets are typical schematic representations of DNW cross-sectional areas in the ⟨0 1 1⟩, ⟨1 1 1⟩ and ⟨0 0 1⟩ crystal orientations.

## 3. Results and discussions

### 3.1. Cross-sectional area dependent thermal conductivity

To study the cross-sectional area dependent thermal conductivity, thermal conductivities of DNWs with different cross-sectional areas ranging from 2 to 30 nm$^2$ have been investigated at 300 K. Three crystal orientations of DNWs have been considered, that is the ⟨0 0 1⟩, ⟨0 1 1⟩ and ⟨1 1 1⟩ crystal orientations. All DNWs lengths considered here are about 85.6 nm. The relationships between cross sectional areas and thermal conductivities for these three crystal orientations of DNWs are shown in Fig. 3. It can be seen that the thermal conductivity increases monotonically with increasing cross-sectional area for these three crystal orientations of DNWs. For the ⟨0 0 1⟩ crystal orientation of DNWs, with increasing cross-sectional areas from 3.9 to 28.2 nm$^2$, thermal conductivities increase from 123.7 to 148.9 W K$^{-1}$ m$^{-1}$. For the ⟨0 1 1⟩ crystal orientation of DNWs, with increasing cross-sectional areas from 2.2 to 20.2 nm$^2$, thermal conductivities increase from 264.9 to 312.1 W K$^{-1}$ m$^{-1}$. For the ⟨1 1 1⟩ crystal orientation of DNWs, with increase in cross-sectional areas from 2.0 to 15.4 nm$^2$, thermal conductivities increase from 177.2 to 240.0 W K$^{-1}$ m$^{-1}$. For the same cross-sectional areas, thermal conductivity for the ⟨0 1 1⟩ orientation of DNWs is larger than for the ⟨1 1 1⟩ orientation of DNWs, and thermal conductivity for the ⟨1 1 1⟩ orientation of DNWs is larger than for the ⟨0 0 1⟩ orientation of DNWs. We also note that thermal conductivities of all DNWs studied here are lower than those of bulk diamond at the corresponding crystal orientation.

To understand the mechanism of cross-sectional area dependence of thermal conductivity, DNWs densities of phonon states in the ⟨0 1 1⟩ crystal orientation have been calculated using the Fourier transform of the velocity autocorrelation function [40], and they are shown in Fig. 4. As can be seen from Fig. 4(a), with the increase in the cross-sectional area, the density of phonon state moves in the lower frequency direction. From phonon kinetic theory, the lattice thermal conductivity can be express as

$$k = (1/3)cvl \quad (6)$$

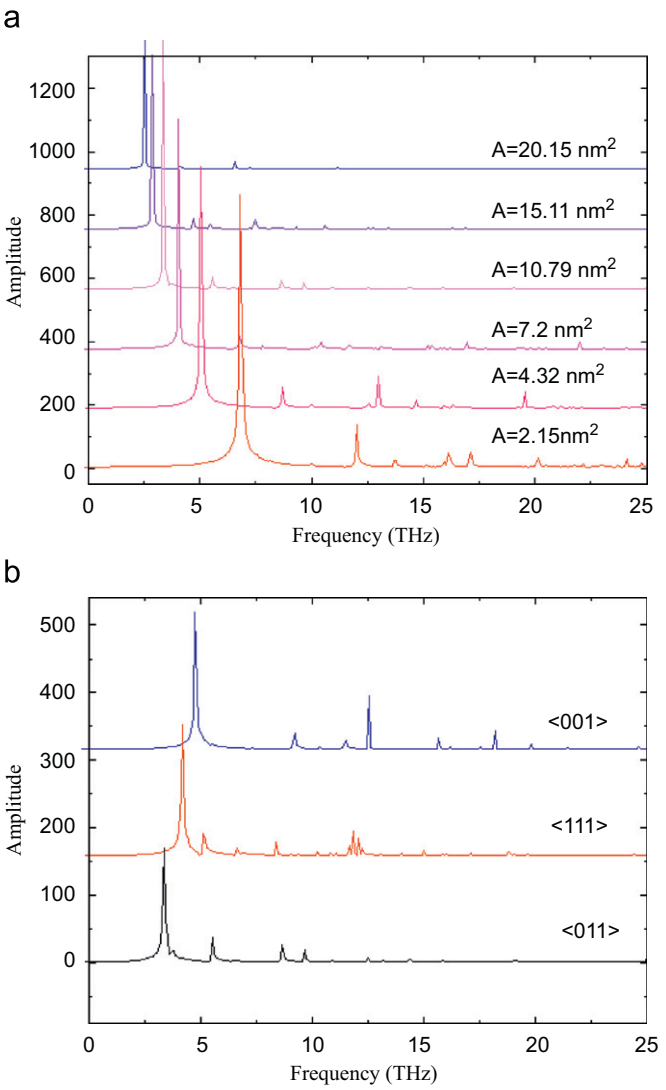


**Fig. 4.** (a) DNW densities of phonon states in the ⟨0 1 1⟩ crystal orientation with cross-sectional areas from 2.15 to 20.15 nm$^2$ and length 85.6 nm at 300 K. (b) DNW densities of phonon states in the ⟨0 1 1⟩, ⟨1 1 1⟩ and ⟨0 0 1⟩ crystal orientations with cross-sectional area 10.15 nm$^2$ and length 85.6 nm at 300 K.

where $c$ is the lattice heat capacity, $v$ the mean velocity of sound and $l$ the phonon mean-free path. The phonon mean-free path depends inversely on phonon frequency [48]. This means that with decrease in phonon frequency, mean free path increases, and phonon–phonon interactions and boundary scattering are reduced, which result in an increase in thermal conductivity. As a result DNW thermal conductivities increase with an increase in the cross-sectional area.

Densities of phonon states for the ⟨0 0 1⟩, ⟨0 1 1⟩ and ⟨1 1 1⟩ crystal orientations of DNWs with cross-sectional area of 10.15 nm$^2$ and length 85.6 nm are shown in Fig. 4(b). As can be seen, the prominent frequency peaks for the ⟨0 1 1⟩, ⟨1 1 1⟩ and ⟨0 0 1⟩ crystal orientations of DNWs are 3.346, 4.225 and 4.771 THz, respectively. This means that the ⟨0 1 1⟩ crystal orientation of DNW has the lowest prominent frequency and longest phonon mean-free path. At the same time, the ⟨0 0 1⟩ crystal orientation of DNW has the highest prominent frequency and the shortest phonon mean-free path. Therefore, thermal conductivity in the ⟨0 1 1⟩ crystal orientation is larger than in other crystal orientations.

### 3.2. Length dependent thermal conductivity

In order to analyze the length effect on thermal conductivity, thermal conductivities of DNWs with length range 26.7–357.1 nm have been computed at 300 K. Three crystal orientations (⟨0 0 1⟩, ⟨0 1 1⟩ and ⟨1 1 1⟩) of DNWs have been considered. All DNWs cross sectional areas have been 2.2 nm$^2$. The relationship between length and thermal conductivity for these three crystal orientations of DNWs are shown in Fig. 5. It can be seen that for the ⟨0 1 1⟩ crystal orientation, thermal conductivity increases from 66.9 to 484.3 W K$^{-1}$ m$^{-1}$ with increase in length range from 26.7 to 354.6 nm. However, for the ⟨0 0 1⟩ crystal orientation, when length increases from 26.75 to 356.68 nm, thermal conductivity increases from 61.53 to 301.92 W K$^{-1}$ m$^{-1}$. In particular, our results show that DNW thermal conductivity in the ⟨0 1 1⟩ crystal orientation is significantly larger than in the ⟨0 0 1⟩ and ⟨1 1 1⟩ crystal orientations. This has also indicated that thermal conductivities in all DNWs considered here are lower than those of corresponding crystal orientations bulk diamond.

In this work, densities of phonon states for the ⟨0 1 1⟩ crystal orientation of DNWs with different lengths from 60 to 320 nm have been calculated, and they are shown in Fig. 6. Our results show that the prominent frequency peak for all DNWs densities of phonon states is around 5.378 THz. With increase in DNW length, the intensity of prominent frequency peak decreases and the phonon mean-free path increases. This implies that phonon scattering and boundary scattering are reduced with increase in DNW length. Therefore, thermal conductivity increases with increase in DNW length.

### 3.3. Temperature dependent thermal conductivity

In this contribution, temperature dependent thermal conductivities of DNWs have been investigated in the temperature range 0–1000 K. All DNW cross-sectional areas studied here have been 2.2 nm$^2$. DNWs with three crystal orientations (⟨0 1 1⟩, ⟨1 1 1⟩ and ⟨0 0 1⟩) and with four different lengths (53, 125, 250 and 320 nm) have been studied. The relationships between temperature and thermal conductivity are shown in Fig. 7. It can be seen that initially thermal conductivities of all DNWs increase with increase in temperature, and then decrease. However, for different

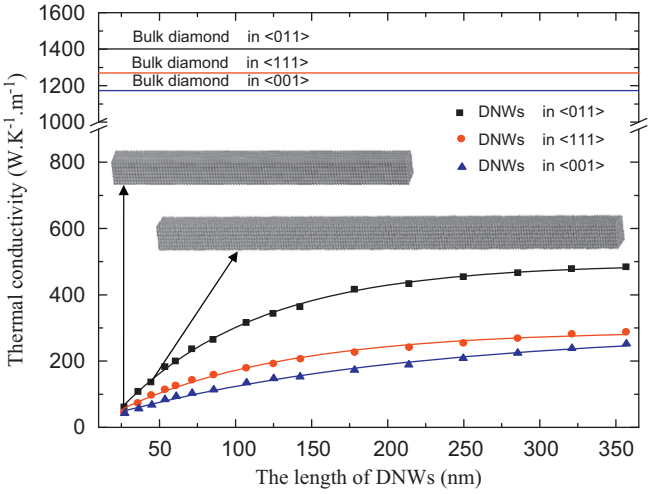


**Fig. 5.** DNW thermal conductivities with length range 26.7–357.1 nm and cross sectional area 2.2 nm$^2$ at 300 K in the ⟨0 1 1⟩, ⟨1 1 1⟩ and ⟨0 0 1⟩ crystal orientations. Also shown are the data of bulk diamond measured for the simulations and schematic representation of the length of DNW. The insets are typical schematic representations of DNW's length in the ⟨0 1 1⟩ crystal orientation.

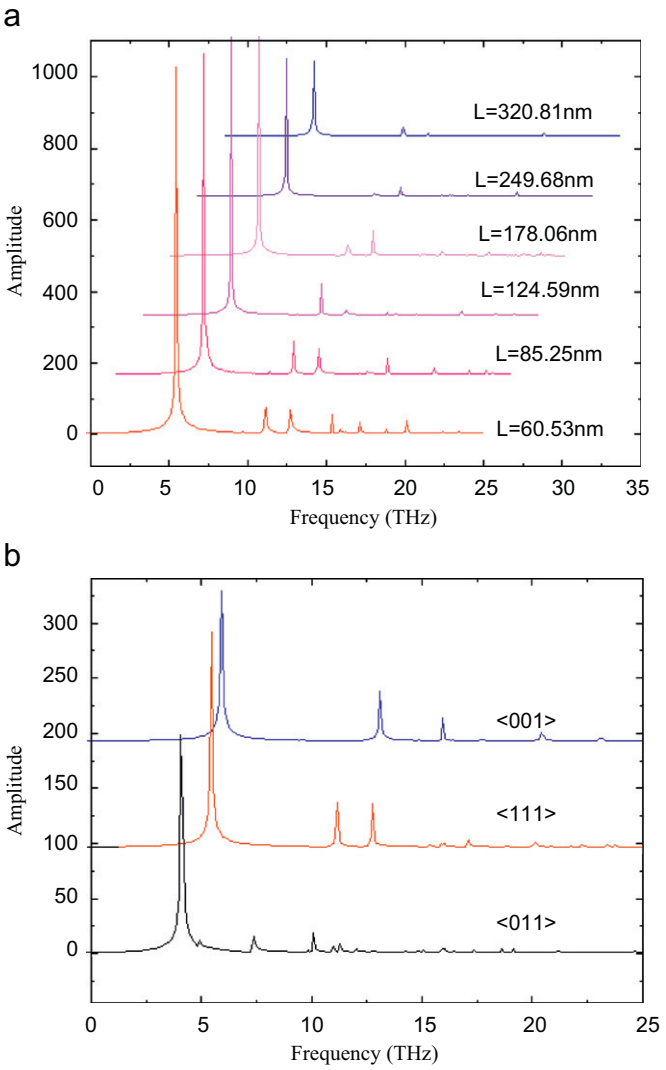


**Fig. 6.** (a) DNW densities of phonon states in the ⟨0 1 1⟩ crystal orientation with lengths from 60.53 to 320.81 nm and cross sectional areas 2.2 nm$^2$ at 300 K. (b) DNW's densities of phonon states in the ⟨0 1 1⟩, ⟨1 1 1⟩ and ⟨0 0 1⟩ crystal orientations with length 213.7 nm and cross sectional areas 2.2 nm$^2$ at 300 K.

lengths and crystal orientations of DNWs, the temperature position for maximum thermal conductivity is different. For all crystal orientations of DNWs, the temperature position for maximum thermal conductivity decreases with increase in DNW's length.

To study the mechanism of temperature dependent thermal conductivity, densities of phonon states have been calculated for the ⟨0 1 1⟩ crystal orientation of DNWs at temperatures 100, 200, 400 and 600 K. The DNWs length is 53 nm and cross-sectional area is 2.2 nm$^2$. As can be seen from Fig. 8, all densities of phonon states have the same prominent frequency peak at 5.413 THz. Moreover, initially the intensities of these prominent frequency peaks decrease with increase in temperature, and then increase. This is why thermal conductivities initially increase with increase in temperature, and then decrease.

## 4. Conclusions

In summary, we have presented non-equilibrium molecular dynamics simulations on geometry and temperature dependent thermal conductivities of diamond nanowires. Our calculated

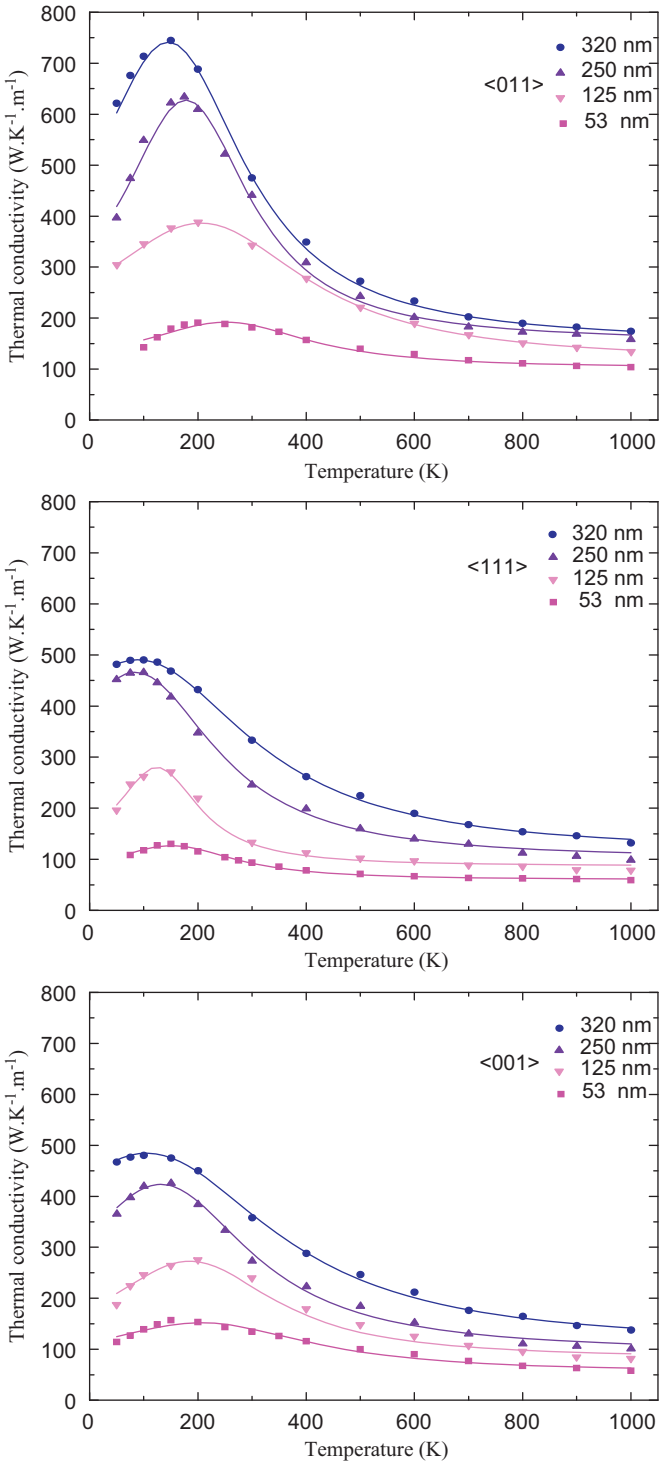


**Fig. 7.** DNW thermal conductivities in the temperature range 0–1000 K in the ⟨0 1 1⟩, ⟨1 1 1⟩ and ⟨0 0 1⟩ crystal orientations with different lengths from 53 to 320 nm and cross sectional area 2.2 nm$^2$.

results indicated that at temperature 300 K, diamond nanowire thermal conductivities increase with increase in length and cross-sectional areas. It is also found that at the same length, temperature and cross-sectional area, thermal conductivities of the ⟨0 1 1⟩ crystal orientation DNWs are larger than those in the ⟨0 0 1⟩ and ⟨1 1 1⟩ crystal orientation DNWs. All diamond nanowires thermal conductivities considered in this work are smaller than those of the corresponding orientations bulk diamond. In addition, in the temperature range 0–1000 K,

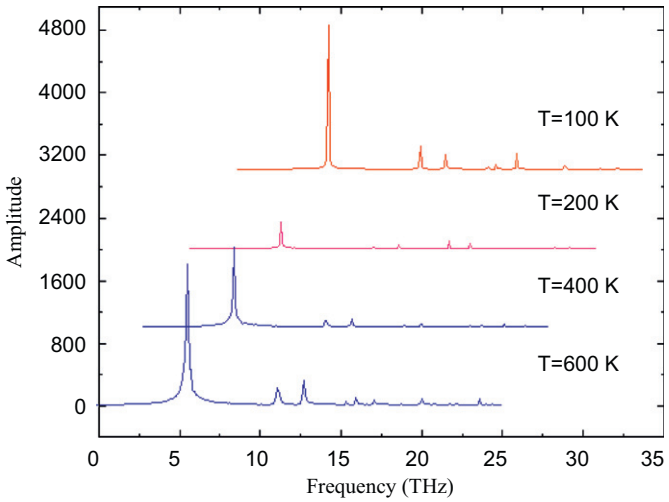


**Fig. 8.** DNW's densities of phonon states at $T=100$, 200, 400 and 600 K with length 53 nm and cross-sectional area 2.2 nm$^2$ in the ⟨0 1 1⟩ crystal orientation.

diamond nanowire's thermal conductivities initially increase with increasing temperature, and then decrease. Geometry and temperature effects on diamond nanowires thermal conductivities can be explained well by calculated densities of phonon states.

## Acknowledgments

This work was supported by the National Natural Science Foundation of China (Grant nos. 50772018 and 50402025) and the Program for New Century Excellent Talents in Chinese Universities (NCET-07-0139). R.M. acknowledges the support from the NSERC and CRC program. This work was made possible by the facilities of the Shared Hierarchical Academic Research Computing Network (SHARCNET), Canada.

## Reference

[1] A.L. Yanson, Nature 395 (1998) 783.
[2] R.H. Baughman, A.A. Zakhidov, Science 297 (2002) 787.
[3] B. Wen, R.V.N. Melnik, Applied Physics Letter 92 (2008) 261911.
[4] D.G. Cahill, W.K. Ford, Journal of Applied Physics 93 (2003) 793.
[5] C.W. Padgett, O. Shenderova, D.W. Brenner, Nano Letters 2006 (1827) 6.
[6] H. Shiomi, Japanese Journal of Applied Physics 36 (1997) 7745.
[7] E.S. Baik, Y.J. Baik, S.W. Lee, D. Jeon, Thin Solid Films 377 (2000) 295.
[8] H. Masudda, M. Watanabe, K. Yasui, Advanced Materials 12 (2000) 444.
[9] Y. Ando, Y. Nishibayashi, A. Sawabe, Diamond and Related Materials 13 (2004) 633.
[10] L.T. Sun, J.L. Gong, Z.Y. Zhu, Advanced Materials 16 (2004) 1849.
[11] L.T. Sun, J.L. Gong, Z.Y. Zhu, Diamond and Related Materials 14 (2005) 749.
[12] Y.S. Zou, Y.T. Yang, W.J. Chong, Applied Physics Letters 92 (2008) 053105.
[13] O. Shenderova, D.W. Brenner, R.S. Ruoff, Nano Letters 3 (2003) 805.
[14] A.S. Barnard, Reviews on Advanced Materials Science 6 (2004) 94.
[15] N. Dubrovinskaia, L. Durbrovinsky, W. Crichton, F. Langenhorst, A. Richter, Applied Physics Letters 87 (2005) 083106.
[16] C.E. Nebel, N. Yang, H. Uetsuka, Diamond and Related Materials 18 (2009) 910.
[17] N.V. Novikov, A.P. Podoba, S.V. Shmegera, A. Witek, A.M. Zaitsev, A.V. Denisenko, Diamond and Related Materials 1602 (1999) 8.
[18] G.Q. Wu, X.R. Kong, Z.W. Sun, Y.H. Wang, Journal of Astronautics 27 (2006) 751.
[19] J.F. Moreland, J.B. Freund, G. Chen, Nanoscale and Microscale Thermophysical Engineering 8 (2004) 61.
[20] J.F. Moreland, J.B. Freund, G. Chen, Proceedings of the Symposium on Micro/Nanoscale Energy Conversion and Transport (2002).
[21] X.B. Li, D.W. Tang, J. Zhu, Journal of the Graduate School of the Chinese Academy of Sciences 25 (2008) 598.
[22] P.K. Schelling, S.R. Phillpot, P. Keblinski, Physical Review B 65 (2002) 144306.
[23] F.A Ercolessi, Molecular Dynamics Primer., Spring College in Computational Physics, ICTP, Trieste, 1997.

[24] S. J. Plimpton, R. Pollock, M. Stevens. Particle-mesh Ewald and rRESPA for parallel molecular dynamics simulations, in: Proceedings of the Eighth SIAM Conference on Parallel Processing for Scientific Computing, Machines, MN, 1997.
[25] J. Teroff, Physical Review B 39 (1989) 5566.
[26] Y.J. Han, H.B. Chae, Physical Review B 52 (1995) 27.
[27] D.G. Onn, A. Witek, Y.Z. Qiu, Physical Review Letters 68 (1992) 2806.
[28] S. Volz, G. Chen, Applied Physics Letters 75 (1999) 2056.
[29] X.G. Liang, B. Shi, Materials Science and Engineering A 292 (2000) 198.
[30] S. Volza, J.B. Saulniera, G. Chenb, P. Beauchampc, Microelectronics Journal 31 (2000) 815.
[31] J. Che, T. Cagin, W.A. Goddard, Nanotechnology 11 (2000) 65.
[32] S. Berber, Y.K. Kwon, D. Tománek, Physical Review Letters 84 (2000) 4613.
[33] S. Maruyama, S. Maruyama, Physica B 323 (2002) 193.
[34] E.G. Noya, D. Srivastava, L.A. Chernozatonskii, M. Menon, Physical Review B 70 (2004) 115416.
[35] C.W. Padgett, D.W. Brenner, Nano Letters 4 (2004) 1051.
[36] Y. Chena, D. Lib, J. Yangc, Y. Wuc, J.R. Lukesd, A. Majumdar, Physica B 349 (2004) 270.
[37] Y. Chen, D. Li, J.R. Lukes, Z. Ni, M. Chen, Physical Review B 72 (2005) 174302.
[38] G. Zhang, B.W. Li, The Journal of Chemical Physics 123 (2005) 114714.
[39] M. Vladkov, J.L. Barrat, Nano Letters 6 (2006) 1224.
[40] I. Ponomareva, D. Srivastava, M. Menon, Nano Letters 7 (2007) 1155.
[41] J.R. Lukes, H. Zhong, Journal of Heat Transfer 129 (2007) 705.
[42] N. Yang, G. Zhang, B.W. Li, Nano Letters 8 (2008) 276.
[43] H.M. Duong, D.V. Papavassiliou, K.J. Mullen, B.L. Wardle, S. Maruyama, Journal of Physical Chemistry C 112 (2008) 19860.
[44] N. Papanikolaou, Journal of Physics: Condensed Matter 20 (2008) 135201.
[45] M.C.H. Wu, J.Y. Hsu, Nanotechnology 20 (2009) 145401.
[46] N.A. Roberts, D.G. Walker, D.Y. Li, International Journal of Heat and Mass Transfer 2009 (2002) 52.
[47] J. Hu, X. Ruan, Y.P. Chen, Nano Letters 9 (2009) 2730.
[48] T.W. Tong (Ed.), Thermal Conductivity, 22, Technomic Publishing Company, Inc., 1994.